Desalination and Water Treatment
www.deswater.com

doi: 10.5004/dwt.2017.21697

99 (2017) 322–329
December

Ionic liquid grafted on layered double hydroxide nanomaterial as a hydrophobic/ion-exchange adsorbent for efficient removal of azo dye

Zahra Tafazoli, Mohammad Saber Tehrani*, Syed Waqif Husain, Parviz Aberoomand Azar

Department of Chemistry, Science and Research Branch, Islamic Azad University, Tehran, Iran,
Fax: +98 2144865166; emails: drmsabertehrani@yahoo.com (M.S. Tehrani), zahra.tafazoli@yahoo.com (Z. Tafazoli), syedwaqifhusain@yahoo.com (S.W. Husain), parvizaberoomand@gmail.com (P.A. Azar)

Received 18 February 2017; Accepted 19 November 2017

ABSTRACT

N-methylimidazole with hydrophobic groups in its structure was immobilized on the interlayer of the layered double hydroxides (LDHs). The LDH/methylimidazolium nanocomposite with high surface area was synthesized and characterized by scanning electron microscopy, thermogravimetric analysis, X-ray diffraction and Fourier transform infrared. This novel hybrid nanostructure was used as a highly efficient sorbent for removal of methyl orange from water. The LDH–dodecyl sulfate was synthesized by coprecipitation method, and next, the ionic liquid was grafted in the inner surface of LDH by sol-gel route. Effects of temperature, removal time, pH, stirring rate, desorption temperature and time on the removal were optimized. The experimental data of isotherm followed the Langmuir isotherm model and the Freundlich model. This research shows that the LDH/methylimidazolium nanocomposite could be utilized as an efficient, ease separable and stable adsorbent for azo dyes.

Keywords: Layered double hydroxide; Ionic liquid; Removal of dye; Azo dye; Nanocomposite

1. Introduction

Ionic liquids (ILs) are a type of salt that are liquid at low temperature (<293 K). ILs are entirely composed of ions (organic cations and either organic or inorganic anions), which have melting points below the conventional temperature of 100°C. This new chemical group can reduce the use of hazardous and polluting organic solvents due to their unique characteristics as well as taking part in various new synthesis. Similarly, by attractive advantage of their unique properties, several IL applications have been described, including reaction media for many organic transformations, in separations and extractions, biotechnology, engineering processes, nanotechnology and so on [1–5]. Moreover, ionic liquids have good extractability for frequent organic compounds and metal ions, mainly depend on their unique structures. But, despite the remarkable application of ionic liquids, these systems frequently require large amounts of ionic liquids that may hinder their widespread practical implementation. Consequently, from both economic and technical standpoint, the productivity of the reaction based on bulk ILs is impeded since a great part of ionic liquid is not contributing in the overall process. To address these essential limitations, immobilized ionic liquids offer many advantages over homogeneous IL systems, such as easy handling and recyclability [6–8]. While, these approaches decrease the amount of ionic liquid applied in a typical process relative to homogeneous systems, leaching of ionic liquid from the heterogeneous support is commonplace. Among these supports, different nanoparticles, polymers and silica can be mentioned. Layered double hydroxides are one of the supports that immobilizing of ILs on LDHs exhibits unique properties.

LDHs are composed of positively charged brucite-like hydroxide layers with an interlayer space in between filled

* Corresponding author.

with charge-compensating anions. LDHs have a general formula of $[M^{2+}_{1-x}M^{3+}_{X}(OH)_2]^{x+}[A^{n-}]_{x/n}\,mH_2O$. M^{2+} and M^{3+} are divalent and trivalent metal ions giving a net positive charge to the sheets, A^{n-} is hydrated anion balancing the charge of the sheets [9,10]. Ability to change all three components of the formula provides a quite rich portfolio of LDHs suitable for many applications such as adsorbents, catalysts, pharmaceutics, ion exchangers, catalyst supports and so on [11–13].

The potential case can greatly accelerate the intercalation of organic molecules grafted into the LDHs interlayer space and improve the chemical–physical properties of the resulting materials. Modified substrates with organic materials results in the surface property change from hydrophilicity to hydrophobicity and shift of the interlayer anions to form organo-LDHs with enlarged interlayer spaces.

In this research, for the first time we report interlayer surface modification of LDH with ionic liquids and have found that our designed- and modified-LDH with IL shows high efficiency adsorption effects for the removal of azo dyes from aqueous solution. At this point, it is believed that the merging of LDHs and ILs providing organic–inorganic hybrid nanocomposite that can open new branch toward to expanding separation, extraction and removal techniques. For this purpose, methyl orange (MO) was tested as model azo compound in water samples. The factors that influenced on the extraction efficiency of anionic pollutant compound including amount of sample, temperature and time of removal and pH were investigated and optimized.

2. Experimental setup

2.1. Chemicals and reagents

$MgCl_2.6H_2O$, $AlCl_3.6H_2O$, sodium dodecyl sulfate (SDS), cetyltrimethylammonium bromide (CTAB), N-methylimidazole, (3-chloropropyl)trimethoxysilane (CPTMS), sodium hydroxide, dichloromethane, MO and all chemical solvents were obtained from the Merck company (Darmstadt, Germany, www.merck.de). The stock solution of anionic compound was prepared in deionized water with a concentration of 200 ppm. The working solutions of above compound were prepared by diluting the stock solution with water, and more diluted working solutions were prepared daily by diluting these solutions with deionized water. All solvents used in this study were of analytical reagent grade.

2.2. Characterization

Scanning electron microscopy (SEM) images were obtained using a Mira 3 XMU instrument. Fourier transform infrared (FT-IR) spectra of the materials were recorded over the range of 400–4,000 cm^{-1} region by using a Thermo Nicolet model Nexux 870 FT-IR spectrometer using the KBr disc method with a 1% sample in 200 mg of spectroscopic-grade KBr. Powder X-ray diffraction (XRD) patterns were recorded in the range of 2°–70° on a Rigaku, Japan, X-ray diffractometer, using Cu Kα radiation (λ = 1.5418 Å) at 40 kV and 40 mA. The absorbance of MO was measured by UV–Vis spectroscopy (CARY100, model: VARIAN). Thermogravimetric analysis (TGA) was carried out using a simultaneous TG apparatus (Linseis model L81A1750 Germany).

2.3. Synthesis of adsorbent

2.3.1. Synthesis of the organic precursor

Synthesis of 1-(3-trimethoxysilylpropyl)-3-methylimidazolium chloride: A mixture of N-methylimidazole (25 mmol) and (3-chloropropyl)trimethoxysilane (25 mmol) was heated at 80°C for 72 h. The unreacted materials were washed by diethyl ether. The resulting liquid was dried under reduced pressure at room temperature.

2.3.2. Synthesis of LDH nanostructure

The Mg/Al-DS LDH precursor was synthesized with a 3:1 ratio of Mg(II) and Al(III) salt together with SDS as an intercalated anion. The synthesis was carried out by the coprecipitation method under a constant pH similar to that reported previously [14]. The pH value of 65 mL aqueous solution containing $MgCl_2.6H_2O$ (0.03 mol), $AlCl_3.6H_2O$ (0.01 mol) and SDS (0.02 mol) was adjusted to about 10 with 8 M NaOH aqueous solution. The obtained slurry was aged for 48 h at 80°C, then filtered and washed with distilled water. The white Mg/Al-DS LDH powder was obtained by drying at 60°C in an oven.

2.3.3. Synthesis of LDH/IL organic–inorganic hybrid nanostructure

30 mL of dichloromethane was added to 5 g of CTAB and stirring for 1 h at 50°C. 15 g of N-methylimidazole-IL and 4 g of Mg/Al-DS LDH precursor were added to 30 mL of dichloromethane and stirring for 1 h. After that, the CTAB solution containing dichloromethane was added to the mixture of N-methylimidazole-IL and Mg/Al-DS LDH. The whole mixture was allowed to react under nitrogen atmosphere for 48 h at 50°C. Finally, the product was filtered and washed thoroughly with water and ethanol. The obtained LDH/IL organic–inorganic hybrid nanostructure was dried at room temperature. The schematic diagram for the preparation of LDH/IL organic–inorganic hybrid nanostructure is shown in Fig. 1.

2.4. Dye adsorption

Adsorption behavior was studied by a batch method, which permits convenient evaluation of parameters that influence the adsorption process such as adsorbent dose, contact time, initial concentration, solution pH and reaction temperature. A series of aqueous solutions of MO with the same pH and their concentration ranging from 5 to 200 mg/L were prepared by dissolving pure analytes in double-distilled water. In each adsorption experiment, 0.05 g

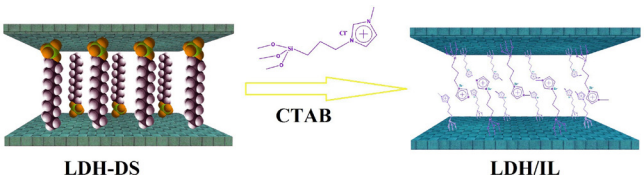

Fig. 1. Schematic representation of the synthesis of LDH/IL organic–inorganic hybrid nanostructure.

adsorbent was added in 50 mL MO solution stirred continuously at constant temperature to observe the effect of pH, MO with the same initial concentration was adjusted to different pH (3–12) using 0.1 mol/L NaOH and 0.1 mol/L HCl solutions. To study the effect of temperature, the adsorption was carried out at different temperatures (25°C, 30°C, 40°C, 50°C and 65°C) and for contact time studies the samples were taken at predetermined time intervals (0.5, 1, 2, 5, 7 and 10 min). After adsorption, the solution was filtered and the amount of non-adsorbed dye ions remaining in the solution was determined spectrophotometrically through UV–Vis spectrophotometer at a wavelength of 463 nm (CARY100, model: VARIAN). The removal efficiency and the amount of dye adsorbed were given according to the formula:

$$q_e = \frac{V(C_o - C_t)}{W} \quad (1)$$

$$\text{Removal } \% = \frac{C_o - C_e}{C_o} \times 100 \quad (2)$$

where C_o and C_e (mg/L) are the initial and equilibrium pollutant concentrations in solution, respectively, C_t (mg/L) is the concentration of MO at time (min), V (L) is the volume of MO solution, W (g) is the mass of nanocomposite adsorbent, q_e (mg/g) is the adsorbed amount at time (min).

3. Results and discussion

3.1. Choice of materials

In our approach, LDH was used as a proper substrate owing to its non-toxicity, ease of availability, antibacterial effect, low cost and so on. The ionic liquid anion exchange properties of the counter ions could be capable of anion exchange. The adsorption of the LDH/IL than raw LDH can be improved. Adsorption mechanism of LDH/IL onto MO is shown in Fig. 2.

In order to increase the selectivity and improve the sorption properties of LDH/IL as an adsorbent, it was used as the substituent on the imidazole ring in the ionic liquid. Therefore, there is an expectation that it efficiently extracts dye compounds easily through anion exchange, electrostatic and hydrophobic interactions.

3.2. Characterization of LDH/IL organic–inorganic hybrid nanostructure

The FT-IR spectrum is used to characterize the molecular structures of LDH/IL organic–inorganic hybrid nanostructure. Fig. 3 shows the FT-IR spectra of dodecyl sulfate–LDH, LDH/IL organic–inorganic hybrid nanostructure and Im–IL in the range of 400–4,000 cm^{-1}. The FT-IR analysis of the dodecyl sulfate–LDH and LDH/IL organic–inorganic hybrid nanostructure exhibits basic characteristic peaks at approximately 584 and 635 cm^{-1} that were attributed to the presence of metal–oxygen bonds stretching vibration. In Im–IL and LDH/IL organic–inorganic hybrid nanostructure spectra, the presence of peaks at 990–1,200 cm^{-1} were most probably owing to the symmetric and asymmetric stretching vibrations of framework and terminal Si–O groups and at 700–790 cm^{-1} for C–Si stretching vibrations, respectively. In the C–H stretching peaks of LDH/IL organic–inorganic hybrid nanostructure spectrum, a band around 1,058 cm^{-1} is observed due to the stretching of the siloxane bonds (≡Si–O). The band at 1,640 cm^{-1} is associated to the bending of the water molecules, which are adsorbed on the surface of the bare silica by hydrogen bonding with the hydroxyl group and the remaining hydroxide groups in the brucite sheets. The broad band around 3,480 cm^{-1} is due to the stretching of the remaining hydroxyl group on the LDH. Spectrum of imidazolium also demonstrated other absorption peaks at 3,138 cm^{-1} (unsaturated C=H stretching), 2,921 and 2,852 cm^{-1} (aliphatic C–H stretching, CPTMS chains and imidazole), 1,640 cm^{-1} (C=N stretching of the imidazolium ring), 1,570 cm^{-1} (C=C stretching of the imidazolium ring), 1,401 and 1,461 cm^{-1} (C–H deformation vibrations).

The XRD pattern in the range of 2θ = 2°–70° for LDH/IL organic–inorganic hybrid nanostructure is shown in Fig. 4. It displays the typical diffraction peaks of the LDH/IL organic–inorganic hybrid nanostructure which showed two sharp basal reflections that were indexed (003) and (006) reflections confirming a well-crystallized lamellar structure in the materials with 3R rhombic symmetry. The main diffraction peak

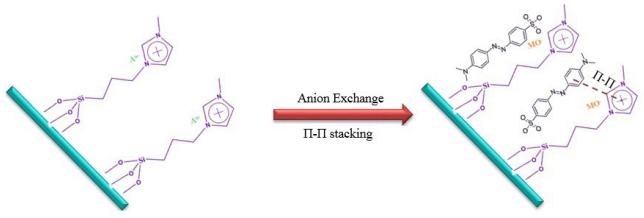

Fig. 2. Adsorption mechanism of LDH/IL onto MO.

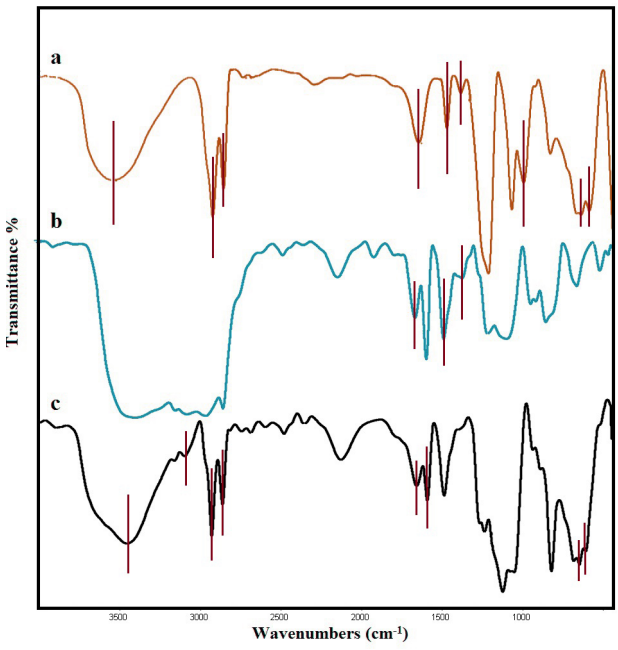

Fig. 3. FT-IR spectra of (a) LDH/IL (b) Im–IL and (c) dodecyl sulfate–LDH.

of LDH/IL is obtained at 2θ value of 2.48°. The d003 spacing of LDH/IL was found to be 2.43 nm, respectively. Allowing for a thickness of 0.48 nm for the brucite-like LDH sheets [15],

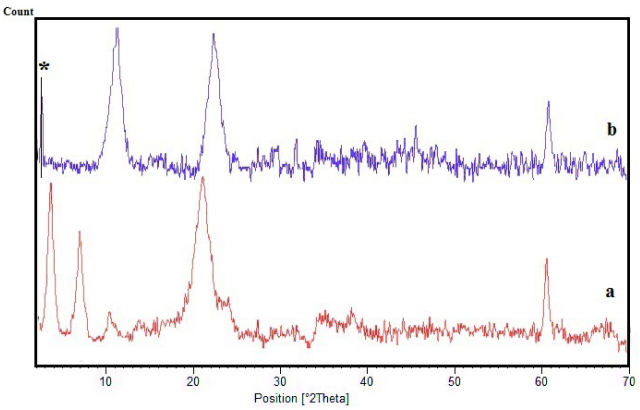

Fig. 4. XRD patterns of (a) dodecyl sulfate–LDH and (b) LDH/IL organic–inorganic hybrid.

the interlayer distance (Δd) of the obtained LDH/IL was estimated to be about 1.95 nm that illustrated covalent interaction between the silanol groups with hydroxyl group on interlayer of the LDH.

Fig. 5(a) clearly shows the dodecyl sulfate–LDH with homogenous structures. Moreover, as it is shown in Fig. 5(b), the LDH/IL organic–inorganic hybrid nanostructures have a homogeneous structure, even after surface modification of dodecyl sulfate–LDH nanostructures with IL groups.

The energy dispersive X-ray (EDX) spectrometry analysis of LDH/IL (Fig. 5(c)) demonstrated the peaks that were associated with Mg, Al, C, N, O, Si and Br atoms with molar ratio of 8.19%, 7.47%, 30.27%, 8.69%, 28.00%, 3.98% and 6.63%, respectively, which confirm the formation of the LDH/IL.

TGA was carried out to investigate further about the interlayer materials present in the galleries of the LDH phase. For sodium IL-functionalized LDH-DS (Fig. 6), the thermal evolution of LDH is characterized by four main steps of weight loss: (a) desorption of physically adsorbed water, (b) dehydration of inter-lamellar water, (c) loss/decomposition of interlayer organic and (d) dehydroxylation of the LDH

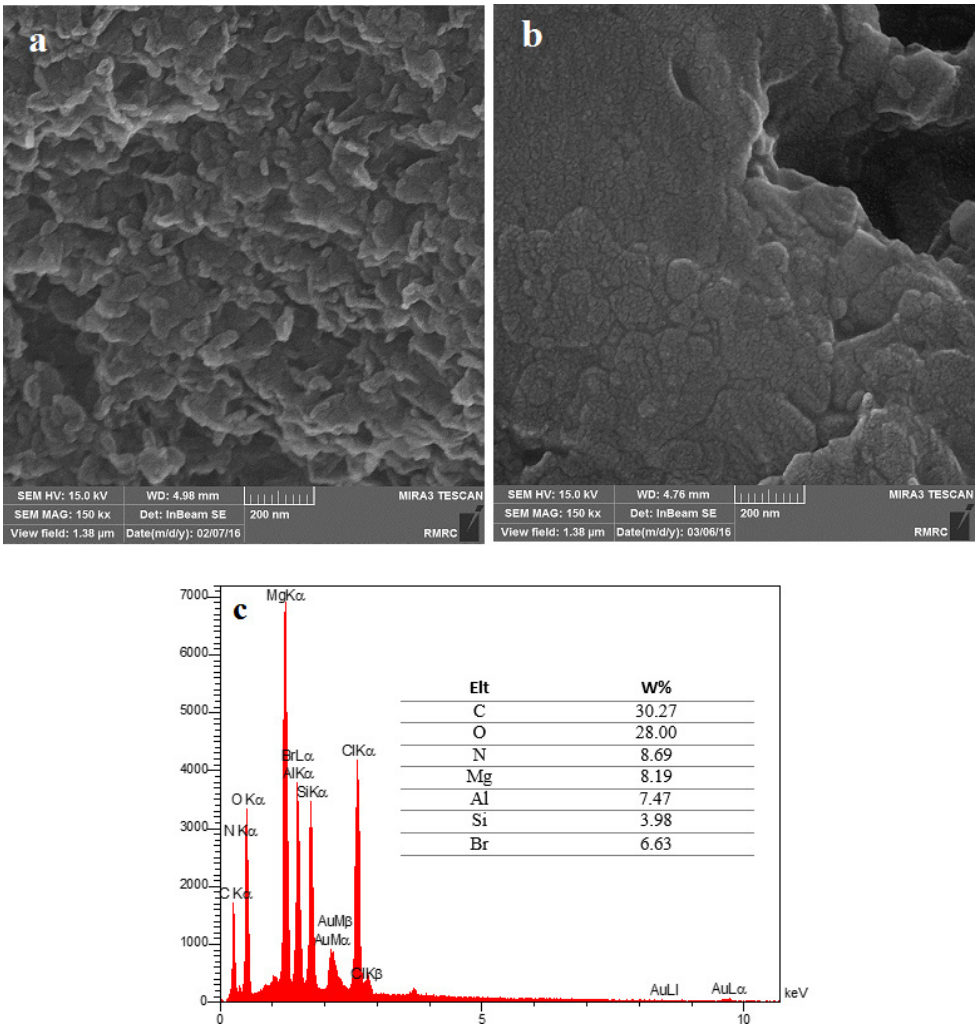

Elt	W%
C	30.27
O	28.00
N	8.69
Mg	8.19
Al	7.47
Si	3.98
Br	6.63

Fig. 5. The SEM images of (a) dodecyl sulfate–LDH and (b) LDH/IL organic–inorganic hybrid nanostructure and (c) EDX of LDH/IL organic–inorganic hybrid nanostructure.

layers, in which some of the steps may overlap. In this way, the first weight loss (about 4.74%) up to 200°C is ascribed to water elimination. Between the temperatures 270°C and 420°C, there is an important weight loss (22.35%) accompanied by a strong exothermic peak associated to the elimination of the interlayer remaining solvent, surfactant and ionic liquid molecules. Another weight loss (15.92%) between 420°C and end can be related to removal of water from the layers dehydroxylation and to a possible release of interlayer bromide anions.

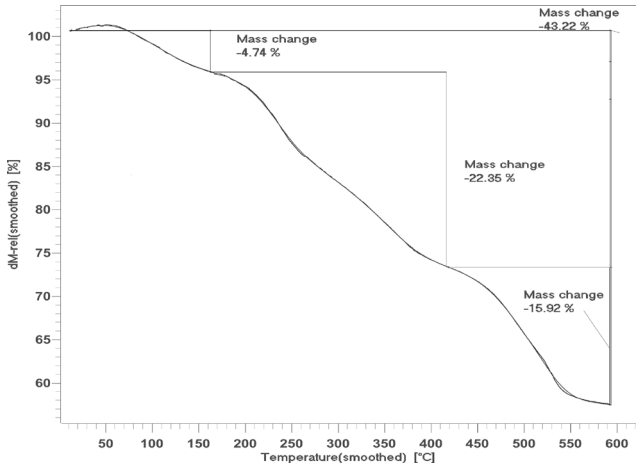

Fig. 6. TGA of LDH/IL organic–inorganic hybrid nanostructure.

3.3. Optimization of the adsorption condition

3.3.1. Effect of adsorbent amount on MO removal

The influence of LDH/IL amount on the adsorption of MO solution is shown in Fig. 7(a). The nanocomposite was tested with various amounts (0.01–0.1 g). The results indicate that by increasing amount of nanocomposite adsorbent, the capability of MO removal was increased, that is because of increasing activated surface. According to Fig. 7(a), an increase occurs when the amount of adsorbent is increased from 0.01 to 0.05. Subsequently, the increased removal percent increases by increasing adsorbent from 0.05 to 0.1, as regards at a lower intensity. Furthermore, the equilibrium amount of adsorbent was investigated to be 0.05 g.

3.3.2. Effect of solution pH on MO removal

The adsorption efficiency of an adsorbent is governed by the solution pH, as it controls the surface charge of the adsorbent. The effect of initial solution pH on MO removal from 50 mg/L of MO solution by 0.05 g of LDH/IL in 5 min is demonstrated in Fig. 7(b). The MO removal efficiency was strongly depended on solution pH and it decreased with increase in pH from 3.0 to 12.0 for all the adsorbents. Specifically, the maximum removal efficiency of 98.4% was observed at pH 7.

3.3.3. Effect of contact time on MO removal

The contact time is one of the important factors affecting batch adsorption process, therefore, contact time from 1 to

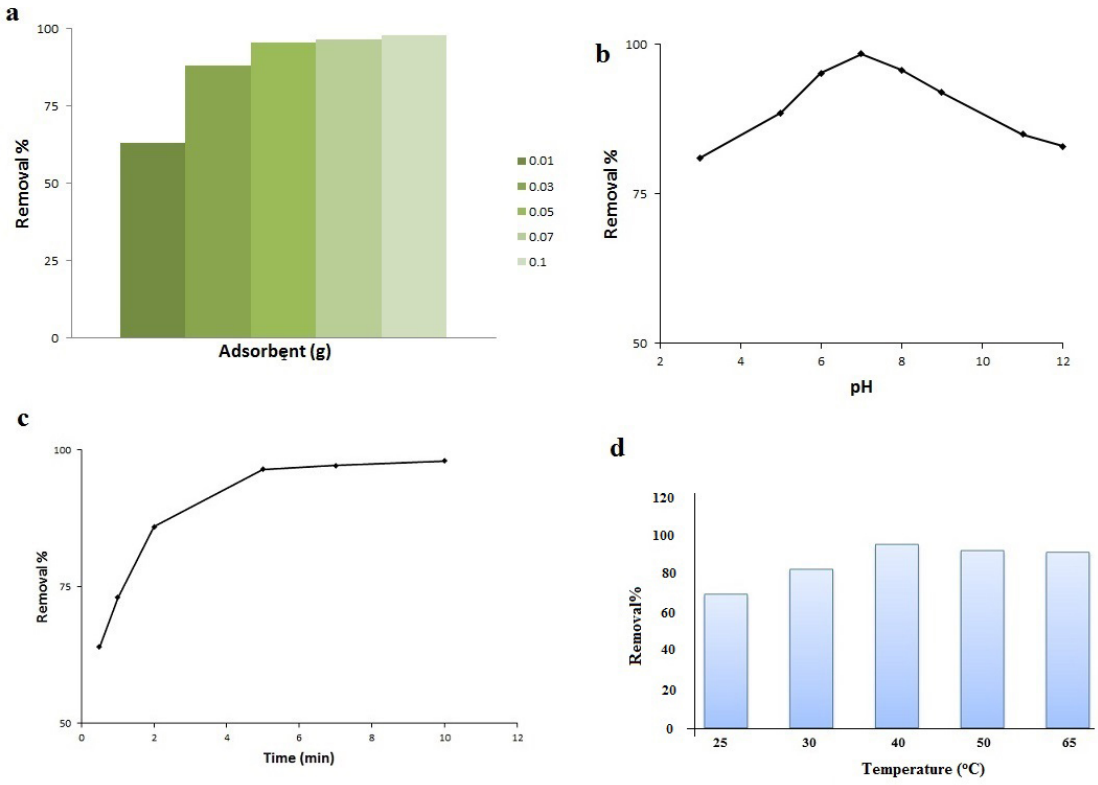

Fig. 7. (a) Effect of adsorbent amount on MO removal. (b) Effect of solution pH on MO removal. (c) Effect of contact time on MO removal. (d) Effect of temperature of dye solution on MO removal.

10 min was studied for removal of dye. Resulting data were shown in Fig. 7(c). This synthesized LDH/IL organic–inorganic hybrid nanostructure adsorbent removed MO very fast, subsequently, that more than 96.5% of dye was removed in 5 min and adsorption process attains saturation at this time.

3.3.4. Effect of temperature of dye solution on MO removal

Dye removal was examined at different temperature range starting from 25°C (as ambient temperature) to 65°C. 50 mL of dye solution 50 mg/L was contacted to 0.05 g of LDH/IL for 5 min at pH 7 at 25°C, 30°C, 40°C, 50°C and 65°C (Fig. 7(d)).

3.4. Adsorption isotherms

In this study, Freundlich and Langmuir isotherms were used to describe the equilibrium between dye ions adsorbed onto the adsorbent and dye ions in the solution.

The Langmuir model assumes a monolayer adsorption on a homogenous surface where the binding sites have equal affinity and energy, and no interaction between the adsorbed species.

The linear form of the Langmuir isotherm model is given as:

$$\frac{C_e}{q_e} = \frac{1}{K_L q_m} + \frac{C_e}{q_m} \tag{3}$$

where C_e is the equilibrium concentration of dye (mg/L), q_e is the amount of dye adsorbed per unit weight of the adsorbent at equilibrium concentration (mg/g) and q_m is the maximum adsorption amount of MO per mg of adsorbent (mg/g) and K_L is the Langmuir adsorption equilibrium constant (L/mg).

The Freundlich isotherm assumes that the adsorption of metal occurs on a heterogeneous surface by multilayer adsorption and that the amount of dye adsorbed increases infinitely with increase in concentration [16]. The linearized Freundlich isotherm model is expressed as:

$$\ln q_e = \ln K_F + \frac{1}{n} \ln C_e \tag{4}$$

where K_f and n are the Freundlich parameters, which are related to the adsorption capacity and intensity, respectively.

Langmuir isotherm assumes that intermolecular forces decrease rapidly with distance and this leads to the prediction that coverage of adsorbent by dye ions is of monolayer type. It represents chemisorption on a set of well-defined localized sorption sites, supposing that once a particular site of the sorbent is occupied by a dye ion, no further adsorption takes place at that site. On the contrary, Freundlich isotherm gives an expression encompassing the surface heterogeneity and the exponential distribution of active sites and their energies; it describes the adsorption as reversible and not restricted to the monolayer formation. This isotherm does not predict any saturation of the sorbent surface, so dye concentration in the sorbent will increase with dye concentration increasing in the solution [17].

As can be seen from Fig. 8 and Table 1, the Freundlich isotherm model gave the high R^2 value, showing that the equilibrium data of MO on LDH/IL were best represented by this model. The good fitness of the adsorption data to Freundlich model implies that the adsorption of MO on the LDH/IL is mostly chemisorption by anion exchange. Also, the adsorption capacity of the existing IL group in the nanostructure can be improved by the hydrophobic interaction that shows the fitness of the adsorption data to Langmuir model. Consequently, this nanostructure can be adsorbed through both physical and chemical interaction and force.

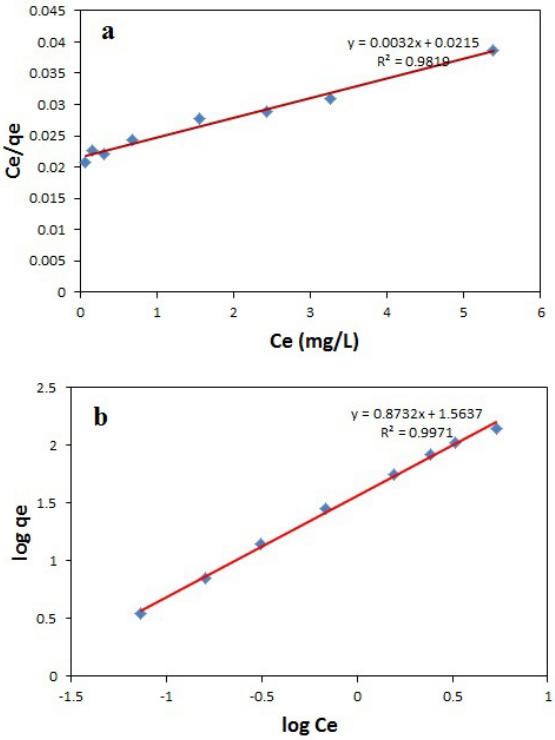

Fig. 8. Adsorption isotherms for MO by LDH/IL organic–inorganic hybrid nanostructure: (a) Langmuir and (b) Freundlich.

Table 1
Parameters of Langmuir's and Freundlich's equation

Langmuir			Freundlich		
Parameters		R^2	Parameters		R^2
K_L (L/mg)	q_m (mg/g)		K_F (L/g)	n	
0.148	312.5	0.9819	7.413	0.639	0.9971

The adsorption capacities of the prepared samples and some previously reported materials for MO are compared (Table 2). The maximum adsorption capacity of LDH/IL on MO is 312.5 mg/g, it could be up to 27 times more than activated rice husk and the synthesized nanohybrid adsorbent developed in this study exhibits very quick adsorption.

4. Conclusion

In this research, the surface of the LDH nanostructures has been modified with N-methylimidazole as ionic liquid group through condensation between the hydroxyl groups and

Table 2
Comparison of different adsorbents for MO adsorption capacities

Adsorbent	Equilibrium time (min)	Initial concentration (mg/L)	Adsorbents dosage (g/L)	Adsorption capacity (mg/g)	References
MCWs	240	50	2	58.82	[18]
K-d-MnO_2 nanosheets	60	500	0.2	145	[19]
Activated rice husk	120	100	50	11.2	[20]
Calcined layered double hydroxides	120	50	1	220	[21]
Chitosan/Fe_2O_3/CNTs	180	40	0.3	66	[22]
Hypercrosslinked polymeric adsorbent	720	100	2.5	70.9	[23]
Activated carbon/Fe_3O_4 nanoparticle composites	180	500	2	303.03	[24]
LDH/IL	5	50	1	312.5	This study

IL groups. Similarly, the LDH/IL organic–inorganic hybrid nanostructure as an adsorbent was used for the removal of MO from water samples. The adsorbent is mechanically stable and exhibits relatively high thermal stability. The construction of the adsorbent is very simple. The experimental data of isotherm followed the Langmuir isotherm model and the Freundlich model. The results indicate that synthesized nanostructure is a technically pragmatic, highly efficient and cost-effective adsorbent for the removal of dye and imply a potential of feasible application for industrial water treatment.

References

[1] Z. Qianli, F. Yang, F. Tang, K. Zeng, K. Wu, Q. Cai, S. Yao, Ionic liquid-coated Fe_3O_4 magnetic nanoparticles as an adsorbent of mixed hemimicelles solid-phase extraction for preconcentration of polycyclic aromatic hydrocarbons in environmental samples, Analyst, 135 (2010) 2426–2433.

[2] W. Eranda, S. Perera, J.A. Crank, L. Sidisky, R. Shirey, A. Berthod, D.W. Armstrong, Bonded ionic liquid polymeric material for solid-phase microextraction GC analysis, Anal. Bioanal. Chem., 396 (2010) 511–524.

[3] X. Liu, X. Lu, Y. Huang, C. Liu, S. Zhao, Fe_3O_4@ ionic liquid@ methyl orange nanoparticles as a novel nano-adsorbent for magnetic solid-phase extraction of polycyclic aromatic hydrocarbons in environmental water samples, Talanta, 119 (2014) 341–347.

[4] Z. Weifeng, T. Yusheng, X. Jia, K. Jie, Functionalized graphene sheets with poly (ionic liquid)s and high adsorption capacity of anionic dyes, Appl. Surf. Sci., 326 (2015) 276–284.

[5] M. Sprynskyy, T. Kowalkowski, H. Tutu, E.M. Cukrowska, B. Buszewski, Ionic liquid modified diatomite as a new effective adsorbent for uranium ions removal from aqueous solution, Colloids Surf., A, 465 (2015) 159–167.

[6] M. Amde, J.F. Liu, L. Pang, Environmental application, fate, effects, and concerns of ionic liquids, Environ. Sci. Technol., 49 (2015) 12611–12627.

[7] M.M. Abolghasemi, B. Karimi, V. Yousefi, Periodic mesoporous organosilica with ionic liquid framework as a novel fiber coating for headspace solid-phase microextraction of polycyclic aromatic hydrocarbons, Anal. Chim. Acta, 804 (2013) 280–286.

[8] B. Karimi, D. Enders, New N-heterocyclic carbene palladium complex/ionic liquid matrix immobilized on silica: application as recoverable catalyst for the Heck reaction, Org. Lett., 8 (2006) 1237–1240.

[9] Q. Tao, J. Yuan, R.L. Frost, H. Hongping, P. Yuan, J. Zhu, Effect of surfactant concentration on the stacking modes of organosilylated layered double hydroxides, Appl. Clay Sci., 45 (2009) 262–269.

[10] C. Domingo, E. Loste, J. Fraile, Calcite precipitation by a high-pressure CO_2 carbonation route, J. Supercrit. Fluids, 36 (2006) 202–215.

[11] K.W. Park, S.Y. Jeong, O.Y. Kwon, Interlamellar silylation of H-kenyaite with 3-aminopropyltriethoxysilane, Appl. Clay Sci., 27 (2004) 21–27.

[12] S.K. Bharqava, B.D. Akolekar, Adsorption of NO and CO over transition-metal-incorporated mesoporous catalytic materials, J. Colloid Interface Sci., 281 (2005) 171–178.

[13] M.M. Abolghasemi, V. Yousefi, M. Piryaei, Double-charged ionic liquid-functionalized layered double hydroxide nanomaterial as a new fiber coating for solid-phase microextraction of phenols, Microchim. Acta, 182 (2015) 2155–2164.

[14] P. Zhang, G. Qian, Z.P. Xu, H. Shi, X. Ruan, J. Yang, R.L. Frost, Effective adsorption of sodium dodecylsulfate (SDS) by hydrocalumite (CaAl-LDH-Cl) induced by self-dissolution and re-precipitation mechanism, J. Colloid. Interface Sci., 367 (2012) 264–271.

[15] E.M. Seftel, M. Niarchos, C. Mitropoulos, M. Mertens, E.F. Vansant, P. Cool, Photocatalytic removal of phenol and methylene-blue in aqueous media using TiO_2@ LDH clay nanocomposites, Catal. Today, 252 (2015) 120–127.

[16] A. Asfaram, M. Ghaedi, S. Agarwal, I. Tyagi, V. Kumar Gupta, Removal of basic dye Auramine-O by ZnS: Cu nanoparticles loaded on activated carbon: optimization of parameters using response surface methodology with central composite design, RSC Adv., 5 (2015) 18438–18450.

[17] Q. Peng, M. Liu, J. Zheng, C. Zhou, Adsorption of dyes in aqueous solutions by chitosan–halloysite nanotubes composite hydrogel beads, Microporous Mesoporous Mater., 201 (2015) 190–201.

[18] R. Lafi, A. Hafiane, Removal of methyl orange (MO) from aqueous solution using cationic surfactants modified coffee waste (MCWs), J. Taiwan Inst. Chem. Eng., 58 (2016) 424–433.

[19] Y. Liu, C. Luo, J. Sun, H. Li, Z. Sun, S. Yan, Enhanced adsorption removal of methyl orange from aqueous solution by nanostructured proton-containing δ-MnO_2, J. Mater. Chem. A, 3 (2015) 5674–5682.

[20] E. Haque, J.E. Lee, I.T. Jang, Y.K. Hwang, J.S. Chang, J. Jegal, S.H. Jhung, Adsorptive removal of methyl orange from aqueous solution with metal-organic frameworks, porous chromium-benzenedicarboxylates, J. Hazard. Mater., 181 (2010) 535–542.

[21] Z.M. Ni, S.J. Xia, L.G. Wang, F.F. Xing, G.X. Pan, Treatment of methyl orange by calcined layered double hydroxides in aqueous solution: adsorption property and kinetic studies, J. Colloid Interface Sci., 316 (2007) 284–291.

[22] H.Y. Zhu, R. Jiang, L. Xiao, G.M. Zeng, Preparation, characterization, adsorption kinetics and thermodynamics of novel magnetic chitosan enwrapping nanosized γ-Fe_2O_3 and multi-walled carbon nanotubes with enhanced adsorption properties for methyl orange, Bioresour. Technol., 101 (2010) 5063–5069.
[23] J.H. Huang, K.L. Huang, S.Q. Liu, A.T. Wang, C. Yan, Adsorption of Rhodamine B and methyl orange on a hypercrosslinked polymeric adsorbent in aqueous solution, Colloids Surf. A, 330 (2008) 55–61.
[24] M.H. Do, N.H. Phan, T.D. Nguyen, T.T. Pham, V.K. Nguyen, T.T. Vu, T.K. Nguyen, Activated carbon/Fe_3O_4 nanoparticle composite: fabrication, methyl orange removal and regeneration by hydrogen peroxide, Chemosphere, 85 (2011) 1269–1276.